

Temporal variability and withinplant heterogeneity in blade biomechanics regulate flowseagrass interactions of *Zostera marina*

*Original*

Temporal variability and withinplant heterogeneity in blade biomechanics regulate flowseagrass interactions of *Zostera marina* / Vettori, Davide; Marjoribanks Timothy, Ian. - In: WATER RESOURCES RESEARCH. - ISSN 0043-1397. - 57:3(2021). [10.1029/2020WR027747]

*Availability:*

This version is available at: 11583/2875025 since: 2021-06-15T10:21:19Z

*Publisher:*

American Geophysical Union

*Published*

DOI:10.1029/2020WR027747

*Terms of use:*

This article is made available under terms and conditions as specified in the corresponding bibliographic description in the repository

*Publisher copyright*

(Article begins on next page)

# Water Resources Research

## RESEARCH ARTICLE

10.1029/2020WR027747

### Key Points:

- Seagrass blade biomechanical traits vary significantly depending on seasonality and blade rank
- Using a simplified numerical model, we investigated the effects of biomechanical variability and heterogeneity on flow-seagrass interactions
- Temporal variability in biomechanics alters light availability and drag force; heterogeneity linked with blade rank enables drag reduction

### Supporting Information:

- Supporting Information S1

### Correspondence to:

D. Vettori,  
[davide.vettori@polito.it](mailto:davide.vettori@polito.it)

### Citation:



Vettori, D., & Marjoribanks, T. I. (2021). Temporal variability and within-plant heterogeneity in blade biomechanics regulate flow-seagrass interactions of *Zostera marina*. *Water Resources Research*, 57, e2020WR027747. <https://doi.org/10.1029/2020WR027747>

Received 20 APR 2020

Accepted 17 FEB 2021

© 2021. American Geophysical Union.  
 All Rights Reserved.

## Temporal Variability and Within-Plant Heterogeneity in Blade Biomechanics Regulate Flow-Seagrass Interactions of *Zostera marina*

D. Vettori<sup>1,3</sup>  and T. I. Marjoribanks<sup>2</sup> 

<sup>1</sup>Geography and Environment, School of Social Sciences, Loughborough University, Loughborough, UK, <sup>2</sup>School of Architecture, Building and Civil Engineering, Loughborough University, Loughborough, UK, <sup>3</sup>Now at Department of Environment, Land and Infrastructure Engineering, Politecnico di Torino, Torino, Italy

**Abstract** Seagrasses are marine flowering plants that have important roles in the ecological and physical processes of many coastal areas. Seagrass modeling to date has mostly assumed that seagrasses have uniform biomechanical traits in space and time. In this study we compare the biomechanical traits of *Zostera marina* blades collected in late summer and spring from a lagoon in southern Denmark. Then, we describe how biomechanics vary depending on (i) seasonality, (ii) storage in laboratory conditions with high nutrient levels, (iii) blade rank and (iv) position along blades. The data collected with these direct measurements are fed into a numerical structural model that simulates seagrass response to an idealized flow and accounts for plant nonuniformity. The model is used to assess the effects of temporal variability and within-plant heterogeneity in blade biomechanics on flow-seagrass interactions. Results show that seagrass biomechanics are affected considerably by seasonality and laboratory storage. This biomechanical variability has a key role in defining flow-seagrass interactions, enhancing light availability in summer and reducing potential drag force in spring. Significant within-plant heterogeneity associated with both blade rank and along-blade position is reported. Compared to temporal variability, within-plant heterogeneity has a secondary role in determining flow-seagrass interactions; however, blade rank is associated with a consistent reduction in the drag force. The results presented improve the understanding of flow-seagrass interactions by clarifying the importance of variations in seagrass blade biomechanical traits and their origin.

## 1. Introduction

Seagrasses are foundation species of many coastal areas worldwide. They provide a variety of ecological services from which key economic value arises (Barbier et al., 2011). Seagrasses create habitats and shelter for benthic organisms and fish, supply food for higher animals (Bakker et al., 2016) and help reducing the number of potential pathogens of marine species and humans (Lamb et al., 2017). They provide a considerable contribution to carbon sequestration (e.g., Duarte et al., 2013) through burial of organic carbon, with an estimated global burial rate of 48–112 Tg C/yr (McLeod et al., 2011). Further, seagrasses significantly influence physical processes in coastal areas by: (i) promoting sediment stability and reducing sediment resuspension (Duarte et al., 2013; Gacia & Duarte, 2001; Hansen & Reidenbach, 2012; James et al., 2019); (ii) increasing light availability above the canopy (e.g., Adams et al., 2016); (iii) reducing current velocity (Hansen & Reidenbach, 2012); and (iv) attenuating incoming waves (e.g., Infantes et al., 2012; Lei & Nepf, 2019b). Seagrasses have attracted research from several disciplines, but there remains the need to understand how their important physical and ecological roles arise from their biomechanical traits.

In recent years seagrasses have been widely investigated to assess their interactions with the flow using field campaigns (Hansen & Reidenbach, 2012; Infantes et al., 2012; Paul & Amos, 2011), laboratory experiments with physical models of seagrass (Abdolahpour et al., 2018; Folkard, 2005; Lei & Nepf, 2019b; Stratigaki et al., 2011), and numerical models (Abdelrhman, 2007; Dijkstra & Uittenbogaard, 2010). Developing models of flow-vegetation interactions is challenging because vegetation is flexible and its biomechanical traits, which are required as input data, show intraspecies variation (Vettori & Nikora, 2020).

By coupling a hydrodynamic model and a biomechanical model, Dijkstra and Uittenbogaard (2010) developed a numerical simulation model to describe the dynamic interactions between seagrass leaves and an

unsteady unidirectional flow. To account for large deflections, the blade was divided in multiple elements and the balance of forces was resolved in each segment to obtain an integrated balance along the whole blade. Dijkstra and Uittenbogaard (2010) assumed biomechanical traits along a leaf to be constant and validated the model using laboratory measurements. Luhar and Nepf (2011) developed a theoretical model for buoyant and flexible seagrass leaves in an idealized unidirectional flow. They concluded that blade posture is controlled by two governing dimensionless parameters:

$$C_y = \frac{1}{2} \frac{\rho C_D w U^2 l^3}{EI}, \quad (1)$$

$$B = \frac{(\rho - \rho_s) g w t l^3}{EI}, \quad (2)$$

where  $\rho$  is the fluid density,  $C_D$  is the drag coefficient,  $U$  is the mean flow velocity of the fluid,  $g$  is gravitational acceleration, and the following quantities relate to the seagrass leaves:  $w$  width,  $l$  length,  $t$  thickness,  $I$  moment of inertia,  $\rho_s$  material density, and  $E$  the Young's modulus at bending. The Cauchy number ( $C_y$ ) represents the ratio of hydrodynamic drag to the restoring forces associated with flexural rigidity. The buoyancy parameter ( $B$ ) is the ratio of the restoring forces due to buoyancy and those due to flexural rigidity.

Blades have a central role both in biological and physical processes involving seagrasses. On the one hand, photosynthetic processes that power seagrass physiology occur within blades; on the other hand, blades are the largest part of plants exposed to the flow, thus they contribute considerably to the total drag force. It follows that aquatic plants have to compromise between maximizing their photosynthetic capacity and minimizing drag force. Earlier works have reported that light irradiance is positively associated with seagrass growth and blade size (e.g., Moore & Wetzel, 2000; Ochieng et al., 2010). Previous research has demonstrated that environmental conditions, such as nutrient availability and seasonality, and hydrodynamic forcing induce variability in blade biomechanical traits in *Zostera noltii* (La Nafie et al., 2012; Soissons et al., 2018) and other seagrass species (de los Santos et al., 2013; La Nafie et al., 2013). Recently, de los Santos et al. (2016) have studied the effect of leaf rank on the biomechanical properties of *Posidonia oceanica*. But we are not aware of any previous work with *Zostera marina* in which the potential heterogeneity of biomechanics across blades within a plant and along individual blades have been characterized.

Based upon previous findings, we expect that environmental conditions also affect those biomechanical traits, such as flexural rigidity, that govern flow-seagrass interactions (Equations 1 and 2). Despite observations that blade biomechanical traits vary with seasons, ecosystems and within-plant, previous models of flow-seagrass interactions (e.g., Dijkstra & Uittenbogaard, 2010; Lei & Nepf, 2019a) have ignored the effects of such variability and have parameterized plants as bodies with idealized uniform properties. As recently demonstrated in the study of wakes behind saltmarsh plants by Marjoribanks et al. (2019), intraspecific variability can play an important role in flow-vegetation interactions. In the context of seagrass, it is unclear how flow-seagrass interactions are affected by temporal variability and within-plant heterogeneity of blade biomechanical traits. To address this knowledge gap the use of numerical models presents a clear advantage because it enables incorporation of biomechanical heterogeneity.

For this study we used specimens of *Z. marina*, a seagrass species widespread in the North Atlantic and along European coasts and characterized by a sequential formation of individual leaves that results in a series of leaves of increasing age moving outwards (Neckles et al., 1993). The objective of this study is twofold: (a) to determine the effects of four factors on the blade biomechanical traits and (b) to characterize how these factors contribute to regulating flow-seagrass interactions by means of variations in blade biomechanical traits. The factors we considered in the present study are: (1) temporal variability associated with laboratory conditions with high nutrient levels; (2) temporal variability associated with seasonality; (3) within-plant heterogeneity associated with blade rank; and (4) within-plant heterogeneity associated with the position along blades. Assessing the effects of laboratory conditions is important because it allows understanding whether flow-seagrass interactions monitored in laboratory experiments (e.g., in flume facilities) conducted with live seagrass are representative of the natural conditions or are biased by the laboratory settings.

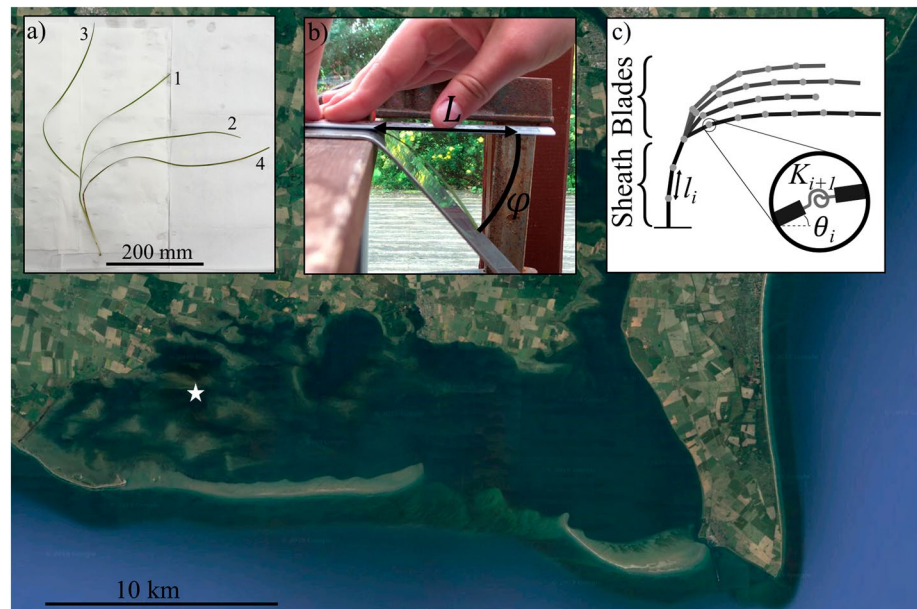


**Figure 1.** Satellite image of the Rødsand lagoon (adapted from Google Earth 2019) with location of DHI’s monitoring station highlighted by a white star. (a) Example of seagrass shoot (collected in August 2017) with leaf ranks reported. (b) Photo of a cantilever test being performed with definitions of cantilever length ( $L$ ) and the angle ( $\varphi$ ) between the flat and inclined parts of the apparatus. (c) Visual representation of the structural model used to study flow-seagrass interactions (not to scale) and detail of the rotational spring between adjacent elements (for description of the parameters see Section 2.4.1). Note that in the structural model the “Sheath” represents the bundle of sheaths present in natural shoots (see lower part of shoot in a) for example).

The objectives of the study are achieved through two main phases: (i) direct measurements of biomechanical traits of seagrass blades exposed to different conditions (e.g., spring and summer) and (ii) numerical simulations by using a structural model to assess flow-seagrass interactions in a unidirectional uniform flow. Biomechanical data collected during phase (i) are used to parameterize the numerical model developed in phase (ii).

## 2. Materials and Methods

### 2.1. Description of the Site

Specimens of *Z. marina* were collected from the Rødsand lagoon (Denmark) in late August 2017 and early April 2018. The Rødsand lagoon is a 30 km by 10 km shallow and sheltered coastal system located south of the Lolland island, in the south of Denmark (Figure 1). The lagoon has a maximum water depth of approximately 8 m and its western (and shallowest) part is home to a healthy community of *Z. marina*. The presence of the seagrass community has been recorded for decades (DHI Denmark, personal communication), from which we infer the environmental conditions in the lagoon are optimal for its growth. The main hydrodynamic forcing in the Rødsand lagoon are currents and wave motion induced by wind, while the effect of tides is weak because of a tidal range of about 0.1 m. Hydrodynamic conditions at the collection site were monitored by DHI Denmark within the remit of Hydralab+ (data available at <https://zenodo.org/record/3529323>). For the hydrodynamic monitoring an acoustic doppler velocimeter (ADV) mounted at a monitoring station (Figure 1) with local mean water depth of 3.4 m was used. The ADV measured at 16 Hz in burst mode, with a sampling period of 17 min and a burst interval of 3 h, and was set above the seagrass canopy so that measurements were taken about 0.5 m below the water surface. For this study we consider a timeseries collected from eighteenth May to 12 June 2017 to obtain a realistic estimate of the mean flow velocity seagrass plants are exposed to at the collection site. In this period of time, which is representative of spring and summer alike, time-averaged horizontal velocity above the seagrass canopy is equal to 0.087 m/s, and the bulk flow Reynolds number is approximately  $10^5$ . Estimates of the environmental

conditions spatially averaged across the lagoon have been obtained from DHI's dedicated ecological model. Between thirteenth and 17 April 2018, the mean values of water salinity and temperature are 9.9 psu and 6.9 °C, respectively, and the light irradiance at the water surface and seabed is 31.3 and 7.3 mol photon/m<sup>2</sup>/d, respectively. Between 29th August and 2 September 2017, the mean values of these environmental parameters are considerably higher: 12.7 psu, 16.4 °C, 47.4 and 12 mol photon/m<sup>2</sup>/d.

## 2.2. Onsite Measurements of Seagrass Biomechanics (Summer)

Seagrass specimens were collected on 29th–31 August 2017 and were stored at ambient temperature in plastic containers filled with seawater retrieved from the site. For simplicity, in the following sections of the manuscript we refer to these specimens as 'summer' specimens. Each specimen consisted of a whole shoot with undamaged leaves (Figure 1a). A total of 15 shoots were used in biomechanical measurements within 48 h of collection, during which time leaf biomechanical traits are expected not to vary (de los Santos et al., 2016). All leaves were cut at the ligule (i.e. at the junction between blade and sheath), then the thickness and width at the top and bottom ends—to obtain an average estimate—the length and the blotted-dry mass of both blades and sheaths were measured using micrometers ( $\pm 0.01$  mm), calipers ( $\pm 0.1$  mm), rulers ( $\pm 1$  mm) and a scale ( $\pm 0.1$  mg), respectively. The material density of each blade and sheath was then calculated using the blotted-dry mass and the volume estimated from morphological measurements. To estimate the flexural rigidity ( $EI$ ) and Young's modulus at bending ( $E$ ) we used a cantilever apparatus developed by Peirce (1930) for the study of textile strips. This technique has been validated against standard engineering tests by Henry (2014) for very flexible materials and has been used to measure the Young's modulus at bending of macroalgae (Vettori & Nikora, 2017) and, more recently, blades of *Z. marina* (Paul & de los Santos, 2019). Where possible, depending on the length of a blade, from each blade a 150–200 mm long sample including the top end and one including the bottom end were used in cantilever tests. To reduce the effect of within-sample material heterogeneity, each sample was tested four times using either end and side, and the mean value from the four tests was retained. The flexural rigidity ( $EI$ ) was calculated using the semi-empirical formula:

$$EI = \frac{mgL^3 \left( \cos(\varphi / 2) \right)}{8l \tan(\varphi)}, \quad (3)$$

where  $m$  and  $l$  are the mass and the length of the sample,  $g$  is the gravitational acceleration,  $L$  is the cantilever length (i.e. the measured parameter), and  $\varphi$  is the angle between the flat and the inclined parts of the apparatus (Peirce, 1930) (Figure 1b). For the cantilever apparatus used in this study  $\varphi = 46^\circ$ . The Young's modulus was obtained as  $E = EI/I$ , where  $I$  is the second moment of area, calculated using the sample width and thickness.

## 2.3. Laboratory Measurements of Seagrass Biomechanics (Spring)

Seagrass specimens were collected on 9 April 2018 and shipped the same day wrapped in newspaper moistened with seawater and surrounded by ice packs. The specimens arrived at the River Science laboratory at Loughborough University (UK), where measurements took place, within 24 h of collection. A total of 95 specimens were used in the experiments, any specimen whose blades looked deteriorated or damaged was discarded. Specimens were arranged into two mesocosms, each of which consisted of a 1 m<sup>3</sup> tank filled with saltwater up to 0.8 m depth and aerated with multiple airstones. The concentration of inorganic nutrients was 234  $\mu\text{mol/l}$  for nitrate, and 4.2–7.9  $\mu\text{mol/l}$  for phosphate. Environmental conditions were designed to replicate those of the Rødsand lagoon in the period in which experiments took place. Hence, seagrass specimens were exposed to a 17h:7 h day-night cycle with light irradiance equal to 60–85  $\mu\text{mol photon/m}^2/\text{s}$  at the bottom of the tank, water temperature ranged from 7 to 8 °C and water salinity was about 10 psu. Light conditions and phosphate concentrations differed slightly between the two mesocosms, namely 60 versus 85  $\mu\text{mol photon/m}^2/\text{s}$  and 7.9 versus 4.2  $\mu\text{mol phosphate/l}$ . However, we verified that both plant health, monitored via chlorophyll fluorescence following standard practices (see supporting information; Baker, 2008; Durako & Kunzelman, 2002; Murchie & Lawson, 2013; Ralph & Burchett, 1995; Ralph & Gademann, 2005), and biomechanical traits were statistically indistinguishable across mesocosms. To test if

seagrass health and biomechanics varied during the laboratory experiments, measurements were conducted across 10 days. On the day seagrass were delivered at the laboratory (i.e. “day 0”) blade biomechanical traits and chlorophyll fluorescence were measured on five specimens, after that, for the following 9 days, the same measurements were performed on five specimens per mesocosm daily.

For measurements of biomechanical traits, blades were removed from the leaves by cutting the leaves at the ligules and ranks were assigned to them starting with the innermost (and youngest) blade and moving outwards (Figure 1a). For each blade we measured the thickness and width at the top and bottom ends, the length and the mass. Differently from the summer specimens, the sheaths of spring specimens were not always intact (due to specimen handling and shipping), therefore measurements were conducted on blades only. Cantilever tests to obtain measurements of flexural rigidity were conducted with samples with a length of 150–200 mm using the technique described in Section 2.2. To investigate biomechanical heterogeneity along blades, samples were prepared including the top and the bottom ends of the blades whenever the blade length allowed it (i.e. blade longer than approximately 300 mm).

## 2.4. Numerical Model of Flow-Seagrass Interactions

### 2.4.1. Structural Model

Seagrass plants were represented in the numerical model using a lumped mass, discrete element method (Figure 1c), with each sheath and blade discretized into a series of elements connected by rotational springs at each joint to represent the effects of rigidity (Marjoribanks & Paul, in press; Neild et al., 2001). This method has been shown to successfully represent the reconfiguration of single shoots with variable geometric and mechanical properties (Marjoribanks & Paul, in press). Here, the model was extended to consider multi-stemmed plants, consisting of a single sheath (representing the bundle of sheaths of a real shoot), with multiple blades connected to its tip. Reconfiguration of the plant was calculated using a relaxed iterative method, by first solving the deformation of the blades assuming an upright sheath. The total force acting on the base of the blades was then summed and applied to the sheath tip and the sheath reconfiguration calculated. The reconfiguration of each of the blades was then recalculated using the new sheath position and this process was repeated until the total Cartesian error between successive blade tip positions for all blades combined was less than 1 mm. Blades were considered independent of each other and therefore the model did not account for blade-blade interaction either through sheltering or collisions.

The internal forcing due to flexural rigidity at each joint between two elements was calculated using a rotational spring, such that the local restoring force was a function of the angle between adjacent elements ( $\theta_i - \theta_{i-1}$ ) and the spring coefficient ( $K_i$ ) which was in turn a function of the local flexural rigidity ( $(EI)_i$ ) and element length ( $l_i$ ), i.e.:

$$K_i = (EI)_i / l_i. \quad (4)$$

The advantage of this approach is that it allows a local expression of the rigidity. Flow-induced external forcing was incorporated through a drag force term ( $F_{D,i}$ ) applied perpendicular to each element  $i$  (Leclercq & de Langre, 2016; Taylor, 1952) while the vertical buoyancy force ( $F_{B,i}$ ) was calculated based on the fluid/vegetation density difference such that:

$$F_{D,i} = \frac{1}{2} \rho C_D l_i w_i U_i^2 \sin^2 \theta_i, \quad (5)$$

$$F_{B,i} = (\rho - \rho_{s,i}) g l_i t_i, \quad (6)$$

where  $\rho$  and  $\rho_{s,i}$  are the fluid and vegetation material densities respectively,  $C_D$  is the drag coefficient, taken as that of a flat plate perpendicular to the flow ( $C_D = 1.95$ ) (Luhar & Nepf, 2011; Vogel, 1981),  $l_i$ ,  $w_i$  and  $t_i$  are the element length, width and thickness respectively, and  $U_i$  is the downstream velocity at the element. While the model can incorporate depth-varying velocity profiles (e.g., Marjoribanks & Paul, in press), the limited field data available were not sufficient to characterize the vertical velocity profile and therefore

the velocity term in Equation 5 was set to a constant value of  $U_i = 0.087$  m/s, representing the conditions measured outside of the vegetation canopy and assuming unidirectional uniform flow. This corresponds to a mean blade Reynolds number of approximately 350. Biomechanical traits were parameterized using the field/laboratory data, with element width and length taken as constant along sheath and blades, while flexural rigidity and thickness varied for some cases (see Section 2.4.2). At each iteration, sheath and blade reconfiguration were calculated by balancing the internal and external forcing terms through solving the steady-state angular equations of motion (full derivation provided in Marjoribanks & Paul, (in press)). It was assumed that each plant was fixed perpendicular to the bed at the base of the sheath and that each blade was joined to the sheath by a spring joint, similar to the elements within both the sheath and blades.

#### 2.4.2. Model Application and Parameterization

Numerical simulations were performed on five different cases: 1) a ‘spring’ case, using biomechanical traits of spring blades pooled independent of their rank and of the position along the blades (i.e. top or bottom) and modeling blades with uniform traits along their length (i.e. width, thickness, material density and Young’s modulus); 2) a ‘summer’ case, using data from summer specimens and modeling blades with uniform traits (as done for the ‘spring’ case); 3) a “laboratory” case, using morphological data of spring specimens, data of the Young’s modulus of blades exposed to laboratory conditions for nine consecutive days and modeling blades with uniform traits (as done for the ‘spring’ case); 4) a “ranked” case, using data of spring specimens according to the blade rank and modeling blades regardless of the position along the blade but accounting for their ranks; and 5) a “heterogeneous” case using data of spring blades pooled independent of their rank but accounting for observed heterogeneity in biomechanical traits along blades (i.e. top vs. bottom). For all cases plants were modeled with four blades, which is the median number of blades present in both spring and summer plants.

For each case, an ensemble of 200 plants were simulated. For each blade of each plant, morphological and mechanical data were generated randomly from the probability distribution of the data collected (Table 1)—it follows that each blade had unique characteristics and within each plant the four blades were different from each other. In doing so, it was assumed that all biomechanical traits were independent. Correlations between all biomechanical traits were weak (values of  $\rho < 0.7$  for Spearman’s rank correlation) and therefore this assumption is satisfactory. For the heterogeneous case, thickness and Young’s modulus data were generated for the base and tip of the blade and a linear profile interpolated along the blade. Correlation between blade base and tip values for biomechanical traits were also weak ( $\rho < 0.46$ ) and therefore they were considered independent. Tests with the cantilever apparatus were not carried out with sheaths and therefore the Young’s modulus for sheaths was based upon the blade value. For cases in which blades are modeled with uniform traits the mean value of the Young’s modulus was used, for the “laboratory” case, the Young’s modulus value is that measured on day 9 of the experiments. For the ranked case the Reuss model was used, and for the heterogeneous case the average of the blade base values of the Young’s modulus was used. The Reuss model allows calculating the Young’s modulus ( $E_{comp}$ ) of composite materials in which the components are aligned normal to the direction of the external force applied (Niklas & Spatz, 2012), such is the case of the bundle of sheaths in *Z. marina*:

$$(E_{comp})^{-1} = \sum_{i=1}^n (V_i / E_i), \quad (7)$$

where  $V_i$  and  $E_i$  are the Young’s modulus and the volume fraction of the  $i$  component (i.e. the four blades). As explained in Section 2.3, it was not possible to measure sheath morphology for the spring specimens and therefore the sheath morphology was assumed to be the same across all conditions.

#### 2.5. Statistical Analysis

Prior to conducting statistical tests, all biomechanical traits were checked for normal distribution with the Lilliefors test and for homogeneity of variance with the Bartlett test for all cases. The dynamics in time of biomechanical traits of spring blades exposed to laboratory conditions was analyzed using 1-way ANOVA on the slope of linear regressions fitted with the least squares method. To assess the effects of the factors under investigation on blade biomechanical traits, the 1-way ANOVA test was used; moreover, differences

**Table 1**  
Distributions of Biomechanical Data Used for the Simulations

Cases	Blade biomechanical traits					
	$l$ (mm)	$w$ (mm)	$t$ (mm)	$\rho_s$ (g/cm <sup>3</sup> )	$E$ (MPa)	
Spring	Weibull $\lambda = 461.5$ $k = 1.78$	Weibull $\lambda = 3.818$ $k = 8.859$	Gamma $\kappa = 32.63$ $\theta = 0.0087$	Gamma $\kappa = 55.45$ $\theta = 0.0166$	Half-normal $\mu = 0.2$ $\sigma = 211.1$	
Laboratory					Half-normal $\mu = 0.64$ $\sigma = 113.3$	
Heterogeneous	Top		Lognormal $\mu = -1.646$ $\sigma = 0.1771$		Half-normal $\mu = 0.2$ $\sigma = 258.1$	
	Bottom		Weibull $\lambda = 0.4042$ $k = 5.767$		Half-normal $\mu = 0.25$ $\sigma = 164.5$	
Ranked	1	Lognormal $\mu = 4.836$ $\sigma = 0.469$	Weibull $\lambda = 3.674$ $k = 9.283$	Gamma $\kappa = 52.68$ $\theta = 0.0044$	Normal $\mu = 0.933$ $\sigma = 0.1176$	Gamma $\kappa = 0.437$ $\theta = 120.9$
	2	Lognormal $\mu = 5.819$ $\sigma = 0.377$	Weibull $\lambda = 3.752$ $k = 9.304$	Normal $\mu = 0.2907$ $\sigma = 0.0352$	Lognormal $\mu = -0.1689$ $\sigma = 0.0913$	Gamma $\kappa = 1.215$ $\theta = 118$
	3	Normal $\mu = 551$ $\sigma = 153.8$	Weibull $\lambda = 3.801$ $k = 9.662$	Weibull $\lambda = 0.3167$ $k = 10.17$	Lognormal $\mu = -0.1072$ $\sigma = 0.1365$	Gamma $\kappa = 2.733$ $\theta = 72.95$
	4	Normal $\mu = 625.3$ $\sigma = 179.6$	Weibull $\lambda = 4.026$ $k = 9.768$	Lognormal $\mu = -1.145$ $\sigma = 0.1254$	Lognormal $\mu = -0.005$ $\sigma = 0.1206$	Half-normal $\mu = 95.9$ $\sigma = 176.3$
Summer	Normal $\mu = 513.7$ $\sigma = 227.2$	Normal $\mu = 4.059$ $\sigma = 0.685$	Normal $\mu = 0.36$ $\sigma = 0.0076$	Lognormal $\mu = -0.1354$ $\sigma = 0.1738$	Gamma $\kappa = 3.494$ $\theta = 72.65$	

associated with blade ranks were tested using Tukey's post-hoc comparisons corrected with the Bonferroni technique.

Flow-seagrass interactions for each case were assessed by analyzing the frequency distributions and the first four statistical moments of plant deflected height (defined as the highest blade tip for a given plant), biomass height (defined as the vertical distribution of plant model elements) and the mean drag force across the ensemble of plants. The spring case was used as the reference case and potential differences in the frequency distributions with all remaining cases were assessed by means of the Kolmogorov-Smirnov test (KS test). We note here that the kurtosis was calculated relative to a normal distribution, namely with a  $-3$  correction.

### 3. Results

#### 3.1. Seagrass Biomechanics

##### 3.1.1. Temporal Variability Associated With Laboratory Conditions

First, it is noted that the slightly different environmental conditions in the two mesocosms (see Section 2.3) did not have any significant effects on the spring blade biomechanical traits (1-way ANOVA:  $p = 0.23-0.77$  for all traits). For this reason, specimens from the two mesocosms were grouped for further analysis.

During the 9-days exposure to laboratory conditions the flexural rigidity ( $EI$ ) and the Young's modulus ( $E$ ) of the spring blades were found to reduce significantly in time ( $F_{1,536} = 31.3$ ,  $p \ll 0.01$  and  $F_{1,536} = 61.7$ ,  $p \ll 0.01$ , respectively), the Young's modulus following  $E$  (MPa) =  $(174 \pm 8) - (11 \pm 1.5)d$  ( $R^2 = 0.103$ ), where

**Table 2**

Comparison of Biomechanical Traits of Blades From Spring and Summer Specimens (Sample Sizes for Morphological Traits: 355 for Spring Blades, 51 for Summer Blades; Sample Sizes for E and EI: 140 for Spring Blades, 75 for Summer Blades)

Blades		Biomechanical traits					
		<i>l</i> (mm)	<i>w</i> (mm)	<i>t</i> (mm)	$\rho_s$ (g/cm <sup>3</sup> )	<i>E</i> (MPa)	<i>EI</i> (Nm <sup>2</sup> )
Spring (pooled)		411 ± 237	3.61 ± 0.483	0.285 ± 0.049	918 ± 124	169 ± 127	8.3 ± 7.9 × 10 <sup>-7</sup>
Summer (pooled)		514 ± 227	4.06 ± 0.685	0.360 ± 0.078	886 ± 154	254 ± 130	2.3 ± 2 × 10 <sup>-6</sup>
1-way ANOVA		F <sub>1,405</sub> = 8.52 <i>p</i> = 0.037	F <sub>1,405</sub> = 34.0 <i>p</i> << 0.01	F <sub>1,405</sub> = 86.8 <i>p</i> << 0.01	F <sub>1,405</sub> = 2.79 <i>p</i> = 0.096	F <sub>1,214</sub> = 21.4 <i>p</i> << 0.01	F <sub>1,214</sub> = 61.8 <i>p</i> << 0.01
Spring	Top		3.66 ± 0.5	0.196 ± 0.038		213 ± 147	8.4 ± 8.4 × 10 <sup>-7</sup>
	Bottom		3.56 ± 0.489	0.374 ± 0.076		134 ± 97	8.2 ± 7.6 × 10 <sup>-7</sup>
1-way ANOVA			F <sub>1,709</sub> = 2.43 <i>p</i> = 0.12	F <sub>1,709</sub> > 100 <i>p</i> << 0.01		F <sub>1,139</sub> = 14.8 <i>p</i> << 0.01	F <sub>1,139</sub> = 0.03 <i>p</i> = 0.86
Summer	Top		4.07 ± 0.607	0.244 ± 0.069		292 ± 97	3 ± 2.4 × 10 <sup>-6</sup>
	Bottom		4.06 ± 0.669	0.476 ± 0.113		220 ± 146	1.6 ± 1 × 10 <sup>-6</sup>
1-way ANOVA			F <sub>1,101</sub> = 0 <i>p</i> = 0.95	F <sub>1,101</sub> = 156 <i>p</i> << 0.01		F <sub>1,74</sub> = 6.1 <i>p</i> = 0.016	F <sub>1,74</sub> = 11.3 <i>p</i> << 0.01

Note: The columns indicate the blade: length *l*; width *w*; thickness *t*; material density  $\rho_s$ ; Young's modulus *E* and flexural rigidity *EI*.

*d* is the number of days the seagrass was kept in the laboratory. All other parameters did not vary significantly with storage time (with  $F_{1,335} \leq 1.48$  and  $p \geq 0.22$ ). Therefore, for further analysis all spring blades data can be grouped, independent of the number of days specimens were stored before measurements, for all parameters but the flexural rigidity and the Young's modulus. This also allows a considerable increase in the size of population to 95 specimens. For the flexural rigidity and the Young's modulus, only values obtained from samples tested in the first three days are used. In this time window the effect of time on *EI* and *E* is not significant ( $F_{1,138} = 0.43$ ,  $p = 0.51$  and  $F_{1,138} = 3.04$ ,  $p = 0.08$ , respectively). Note that by using a smaller time window of two days the effect of time would reduce further, but the sample size would shrink considerably as well.

### 3.1.2. Temporal Variability Associated With Seasonality

The number of photosynthetically active (i.e. green) leaves in each seagrass shoot was similar in spring and summer, with mean values of 3.7 and 3.5, respectively, and medians equal to 4, a typical value for *Z. marina* (Neckles et al., 1993). However, on average summer specimens also had two inactive (brown) leaves. Dimensions of the sheaths were collected for summer specimens only; on average sheath bundles were 200 mm long, with a cross section of 3.55 mm by 1.56 mm and a material density of 1.05 g/cm<sup>3</sup>. No cantilever tests could be conducted successfully on sheath bundles because they were too stiff. To investigate the effect of seasonality on biomechanical traits we compared the pooled data of spring blades and those of summer blades. Results are summarized in Table 2 and indicate that summer blades are larger (in all dimensions) than spring blades. Summer blades are also stiffer and have a marginally lower material density than spring blades. These biomechanical differences indicate that both restoring forces due to stiffness and buoyancy are stronger for seagrass in summer than in spring.

### 3.1.3. Within-plant Heterogeneity Associated with blade Rank

Heterogeneity associated with blade rank was found to be significant for all biomechanical traits considered in this study (Figure 2). All dimensions increase significantly with ascending blade rank, but they appear to reach an asymptote for blade rank four and above, after which no significant variation is evident (Figures 2a–2c). While blade length spans from 100 to 1000 mm across ranks, the ranges of blade width and thickness across ranks are considerably limited. Also the remaining traits increase significantly with ascending blade rank (Figures 2d–2f), even though the material density does not exhibit a trend as clear as the Young's modulus and the flexural rigidity. These trends are consistent with the estimates of material density and Young's modulus obtained from 21 brown (inactive) blades in summer specimens - for which

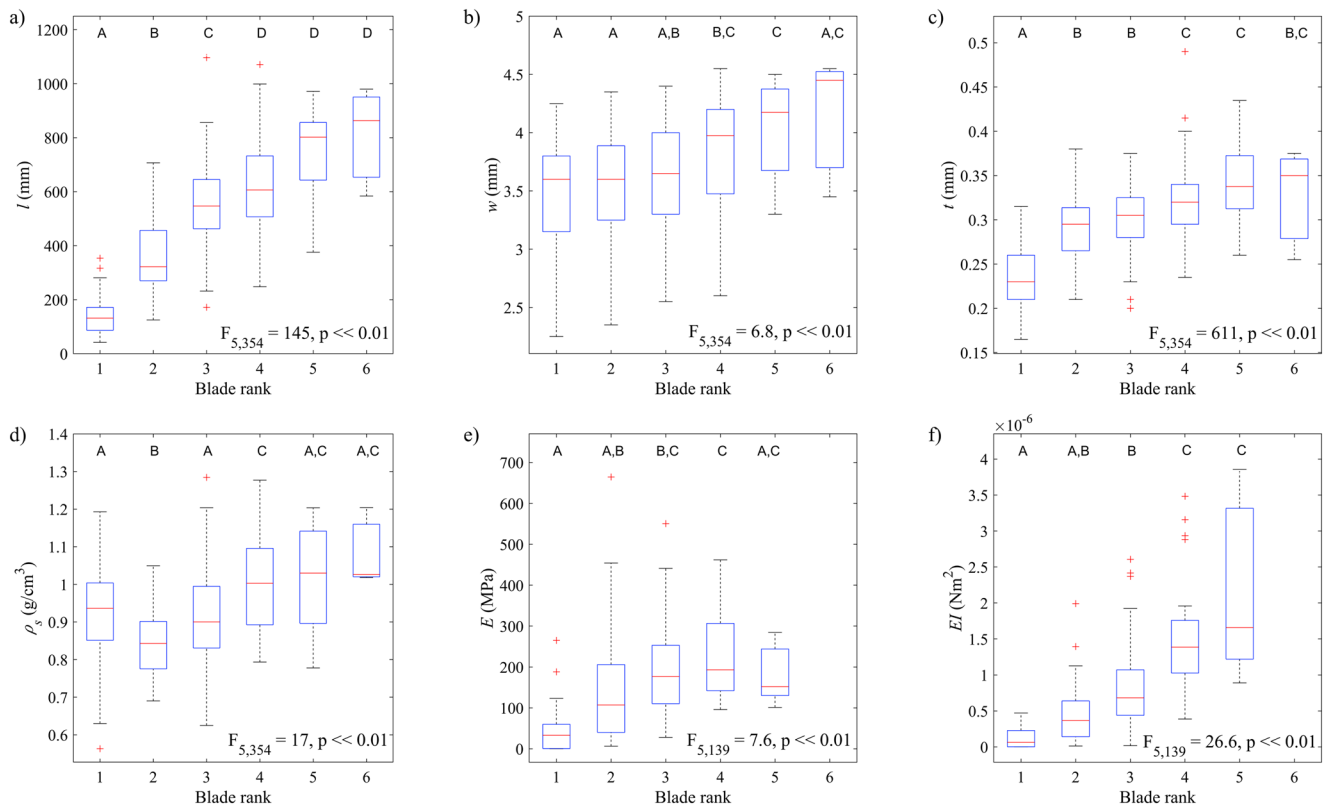


**Figure 2.** Results of Tukey’s post-hoc comparisons corrected with the Bonferroni technique relative to the effects of blade rank on biomechanical traits of spring blades: (a) length; (b) width; (c) thickness; (d) material density; (e) Young’s modulus; and (f) flexural rigidity. Letters indicate the significant differences. Sample sizes for dimensions and material density in blade rank ascending order are: 95, 95, 84, 56, 12, 3. Sample sizes for  $E$  and  $EI$  are limited because only specimens tested in the first three days of experiments were considered in the analysis, in blade rank ascending order they are: 18, 41, 49, 25, 7 (i.e., no measurements from blades with rank 6).

$\rho_s = 1300 \pm 310 \text{ g/cm}^3$ ,  $E = 408 \pm 211 \text{ MPa}$  and  $EI = (3.1 \pm 2.6) \times 10^{-6} \text{ Nm}^2$  - and indicate that blade aging is associated with blades becoming heavier and stiffer.

### 3.1.4. Within-plant Heterogeneity Associated With Position Along Blades

For both spring and summer blades, results indicate that the top part of the blade is stiffer than the bottom part (see values of  $E$  in Table 2). In contrast to this trend, blades are thicker at the bottom in both seasons, while the blade width does not change significantly from top to bottom in either season (Table 2). In light of these contrasting heterogeneities in the blade thickness and Young’s modulus, we consider blade flexural rigidity  $EI$ , which is a key parameter in defining seagrass response to hydrodynamic forcing (Equations 1 and 2). Interestingly,  $EI$  does not vary significantly along blades in spring specimens, while in summer specimens the bottom part is significantly more rigid than the top part (Table 2).

### 3.2. Flow-Seagrass Interactions

The preceding sections identify significant variations in blade biomechanics associated with the effects of the four factors under study. Here we use the numerical simulation of shoot ensembles to identify the impact of these factors on flow-seagrass interactions.

Compared to the spring case, summer shoots are less deflected (KS test,  $p < < 0.01$ ) and their biomass is distributed higher up in the water column (KS test,  $p < < 0.01$ ; Figure 3). The skewness of deflected height is close to zero, meaning that shoots in the summer case have a more symmetric vertical distribution compared to those in the spring case. Further, the variance and the kurtosis of biomass height are at their highest and lowest across the cases investigated, respectively, suggesting that it is more frequent for shoots in

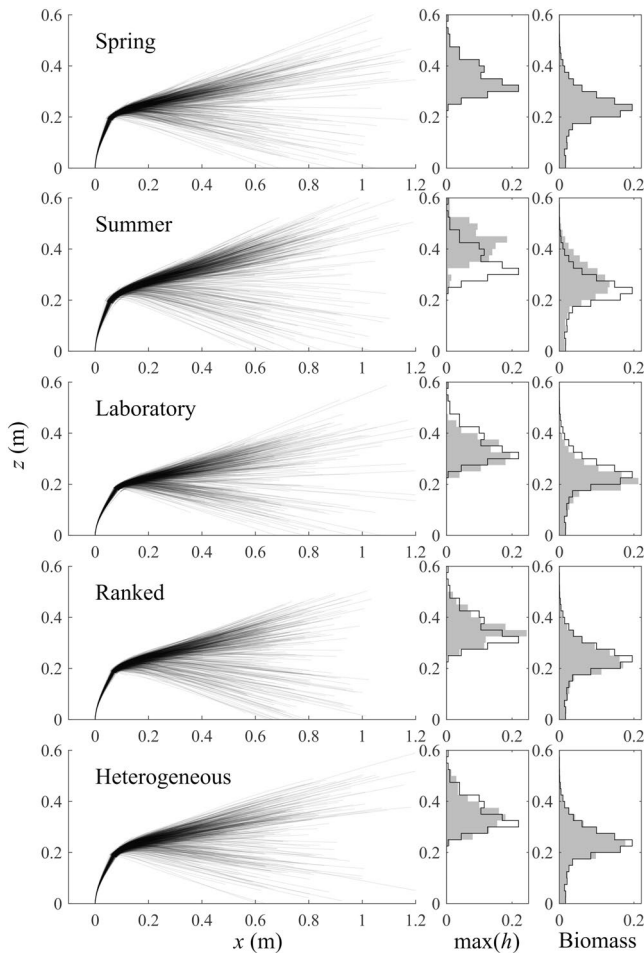


**Figure 3.** Results of numerical models of flow-seagrass interactions: (left panels) plant posture (all 200 simulated plants are displayed); (central panels) frequency distribution of plant deflected height; and (right panels) frequency distribution of plant biomass height. In the central and right panels, the frequency distributions of the spring case are superimposed as a black line for reference.

the summer case to have biomass located high up in the water column. The drag force experienced by shoots in the summer case is considerably higher than that experienced in the spring case (KS test,  $p < 0.01$ ), the mean value being about 45% higher (Table 3). Also, it is interesting to note that the variance of drag for the summer case is considerably higher compared to the other cases investigated, indicating that shoots are exposed to a wider range of drag forces (Figure 4).

The reduction in seagrass flexural rigidity associated with a 9-days exposure to laboratory conditions affects the deflected height significantly (KS,  $p < 0.01$ ) and is associated with a larger portion of the biomass (KS test,  $p < 0.01$ ) being distributed closer to the seabed than in the spring case. This effect is visible on the mean value of the biomass height (Table 3). Consequently, the drag force experienced by plants in the laboratory case is lower than in the spring case (KS test,  $p < 0.01$ ; Table 3) both in its mean value (27% difference) and in its range (Figure 4).

Within-plant heterogeneities associated to blade rank and position along blades (in spring specimens) do not affect seagrass response to hydrodynamic forcing as significantly as temporal variability related to seasonality (Figure 3). On the one hand, the frequency distribution of the deflected height does not differ significantly from that of the spring case (KS test,  $p = 0.05$  and  $p = 0.91$  for ranked and heterogeneous cases, respectively). On the other hand, the biomass vertical distribution for the ranked case varies from that of the spring case (KS test,  $p < 0.01$ ), with seagrass blades being slightly farther from the water surface. Concerning the drag force, both the ranked case and the heterogeneous case have frequency distributions shifted toward lower values (KS test,  $p < 0.01$  and  $p < 0.01$ , respectively; Figure 4) and a mean drag about 10% and 2% lower than that of the spring case, respectively (Table 3). Similar to this trend, also the variance of the drag force is lower than in the spring case. The little effect of within-plant heterogeneity associated to position along blades on seagrass response to hydrodynamic forcing was confirmed by additional simulations performed with the summer specimens (see supporting information).

**Table 3**  
Statistical Moments of Output Parameters From Numerical Models of Flow-Seagrass Interactions

Case	Deflected height (m)				Biomass height (m)				Drag force (mN)			
	Mean	Var	Skew	Kurt	Mean	Var	Skew	Kurt	Mean	Var	Skew	Kurt
Spring	0.354	0.004	1.04	1.47	0.235	0.006	-0.387	1.59	8.21	0.373	0.012	-0.389
Summer	0.421	0.004	0.258	0.613	0.264	0.008	-0.353	0.864	11.9	1.07	0.328	1.22
Laboratory	0.33	0.003	0.954	2.10	0.215	0.005	-0.317	1.47	6.04	0.104	0.727	1.88
Ranked	0.355	0.003	0.521	-0.087	0.228	0.006	-0.491	0.982	7.36	0.17	0.372	0.421
Heterogeneous	0.351	0.004	0.882	1.09	0.235	0.006	-0.349	1.46	8.02	0.271	0.147	-0.115

Note: The unit of measurements of the statistical moments are m or mN for the mean and  $m^2$  or  $mN^2$  for the variance, skewness and kurtosis are dimensionless.

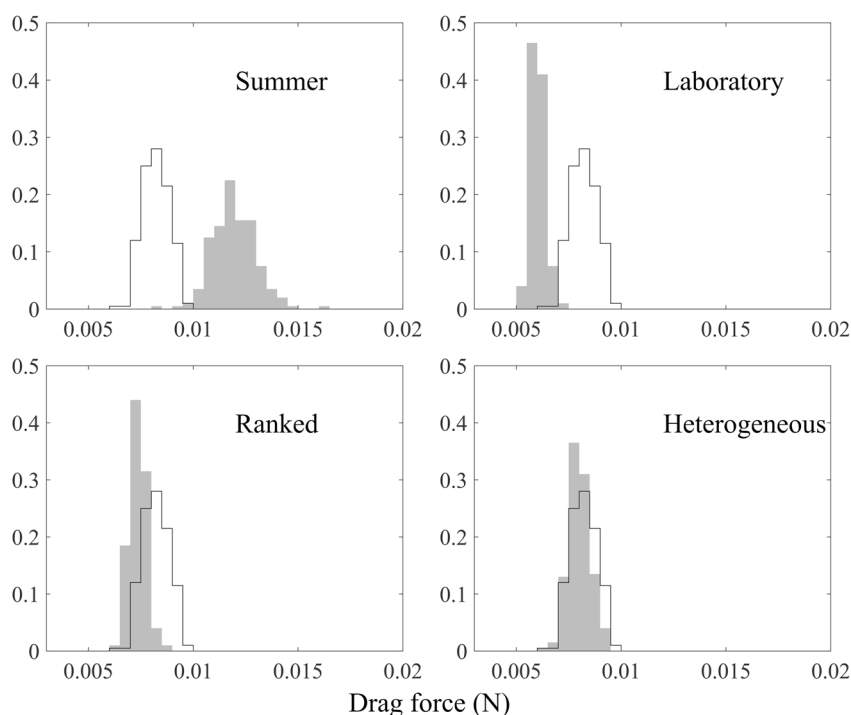


**Figure 4.** Frequency distributions of the drag force: grayed areas are the frequency distributions of the cases reported in panels; black line is the frequency distribution of the spring case used as a reference.

## 4. Discussion

### 4.1. Variability and Heterogeneity in Seagrass Biomechanics

When live vegetation is used in flume facilities (e.g., for investigating its effects on the flow properties), it is important that its behavior is representative of what happens in the natural environment. Our results indicate that in the first 48 h in the mesocosms the biomechanical traits of *Z. marina* did not vary significantly, suggesting that in this time window seagrass response to hydrodynamic forcing is preserved. Interestingly, this finding agrees with what reported by de los Santos et al. (2016) for *P. oceanica*. However, exposure to laboratory conditions for 9 days did reduce significantly the Young's modulus and flexural rigidity of seagrass blades, similarly to what was found by Vettori and Rice (2020) for freshwater macrophytes. This effect was likely caused by the nutrient-rich saltwater used in the mesocosms, with concentration of nitrate and phosphate 5–10 higher than that in the Rødsand lagoon. The environmental model of the Rødsand lagoon estimates concentrations of nitrate and phosphate near the collection site as 18.3–20.4  $\mu\text{mol/l}$  and 0.84–1  $\mu\text{mol/l}$ , respectively (FEMA, 2013). Burkholder et al. (1992) first reported, via qualitative observations, that 4–5 weeks exposure to high levels of nitrate affected the structural integrity of blades of *Z. marina*. More recent studies confirmed that long-term exposure to high nutrient concentration induced a reduction in the tensile Young's modulus of blades of *Z. noltii* (La Nafie et al., 2012; Soissons et al., 2018). Our results agree with previous findings and suggest that even a short-term exposure to nutrient-rich water is sufficient to affect seagrass mechanical properties. According to Ralph et al. (2007), light limitations first affect seagrass physiological response, followed then by morphological changes. Our results indicate that short-term excessive nutrient concentration impacts the mechanical properties of blade tissue, while their physiological status is affected only marginally (see supporting information for results on blade physiological status).

As a consequence of the seasonal cycle, all blade biomechanical traits decreased from late summer to spring except material density, which increased. An effect of seasonality on seagrass blade biomechanical traits was also reported by Paul and de los Santos (2019), de los Santos et al. (2013) and Soissons et al. (2018). Focusing on *Z. marina*, variations in the biomechanical traits reported by Paul and de los Santos (2019) are in general agreement with the findings of the present study, but for a different trend in blade length

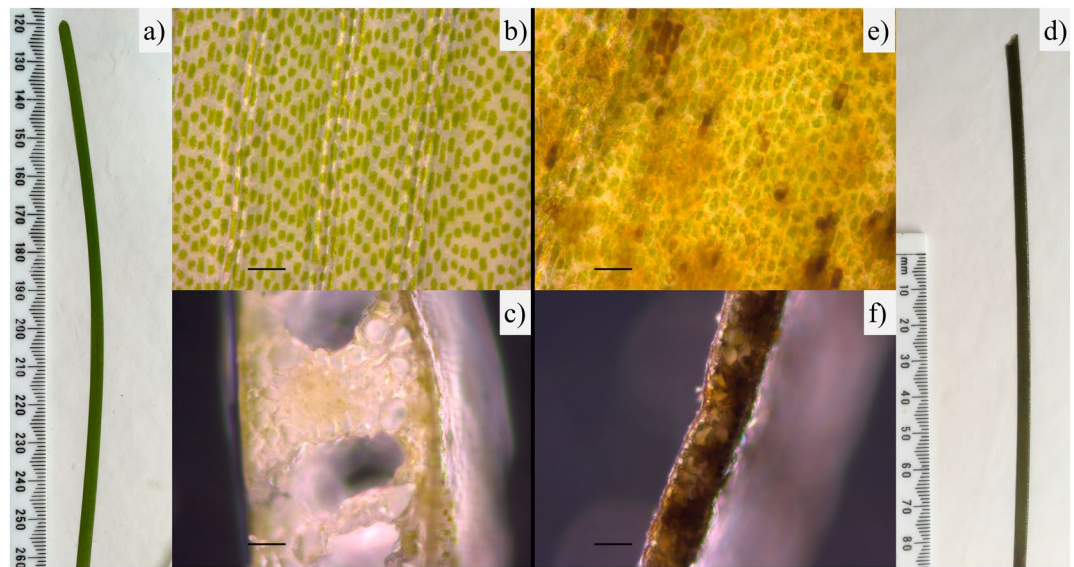


**Figure 5.** Comparison between a healthy blade (a)–(c) and a blade whose distal part is covered by epiphytes (d)–(f) affecting its biomechanics: in (a) and (d) distal blades are shown in their entirety; (b) and (e) display close-ups of the blade surface (note how e) is covered by epiphytes); and (c) and (f) display blades cross-section (in c) large air lacunae are clearly visible). The scale bar in (b)–(c) and (e)–(f) is 0.1 mm.

that they related to the particularly hot climate at their study site. Our findings indicate that over summer blades can maintain a more upright posture than in spring, hence potentially boosting the amount of light available (this was confirmed by analysis of flow-seagrass interactions results, see Section 4.2). The cause of these differences in summer blades is likely to be two-fold: (i) larger air lacunae (Figure 5c) within leaf tissues, also associated with thicker blades, that guarantee greater buoyancy (Hemminga & Duarte, 2000); and (ii) older blades whose tissues become stiffer as they age, similar to what reported by Niklas (1992) for most plant species.

Aging of blade tissues is associated with variations in the Young's modulus even within individual blades. In *Z. Marina* blades grow basally from the upper side of the rhizome nodes, thus the oldest tissues are found on the top (distal) part of the blade (Kuo & Den Hartog, 2007). Consequently, the top part of the blade has a Young's modulus considerably higher than the bottom (basal) part. Moreover, distal parts being thinner than basal parts may be associated with the presence of epiphytes (Figure 5e). In this study epiphytes were only found in the distal parts of blades, and previous studies on *Z. marina* reported that parasites can induce filling of air lacunae (Figure 5f) and reduction of buoyancy in blades (e.g., Hily et al., 2002). Therefore, we deduce that reduction in blade thickness and strong presence of epiphytes in blade distal parts are correlated.

All blade biomechanical traits increased with blade rank (Figure 2), even though there is no significant growth from blade rank 4 onwards. A reason for this might be the limited amount of blades with rank 5–6 analyzed. Alternatively, we suggest that blade biomechanical traits show an asymptotic trend with age: when blades exceed a certain age (associated with rank 4, which is also the median number of blades in a plant in both seasons) their biomechanical traits do not change. This may be related to external biotic factors such as grazers and epiphytes on the blade surface. For example, the length of blades with rank five and six was not significantly different than that of blades with rank 4 (Figure 2a), but blades with rank five or six were often damaged on their distal part, indicating that they would have been longer in the absence of external factors. In contrast to blade length, blade width displayed small increments across blade ranks (Figure 2b). This is related to how seagrass blades are developed, with older blades (i.e. with higher ranks) enclosing younger blades in a protective bundle of sheaths (Kuo & Den Hartog, 2007). Blade thickness increases significantly from blade rank one to four and stabilizes for higher ranks (Figure 2c). This seems to be related with the strong presence of epiphytes on the surface of older tissues, in this case older blades (Figures 5e and 5f). Neckles et al. (1993) reported a strong correlation between the magnitude of epiphyte

cover on blades and blade age in *Z. marina*. The fact that blades with rank above four do not get thicker is also linked with the trend in blade material density (Figure 2d), with blades becoming less buoyant as they get older. This guarantees that old blades sink to the seabed, preventing self-shading of younger blades. Lastly, both the Young's modulus and the flexural rigidity display a significant increase across blade ranks (Figures 2e and 2f) due to blade tissues becoming stiffer as they age. Our findings are quite different from those on *P. oceanica* available in the literature (de los Santos et al., 2016), according to which mid-aged leaves are the largest and leaves weaken and lose stiffness with age. These differences may be associated with the different ecosystems—*P. oceanica* was sampled in the Mediterranean Sea—, different species, or the fact that samples of *P. oceanica* were collected in early summer.

#### 4.2. Effects on Flow-Vegetation Interactions

It is worth recalling here that our numerical model makes use of simplified hydrodynamic conditions which do not reflect the unsteady hydrodynamic forcing that seagrass experience at the collection site. In particular, while our model considers an idealized steady flow with uniform velocity across the vertical profile, seagrass grew exposed to combined wave-current flows. Moreover, the variations in flow-seagrass interactions reported in the present work may be of limited magnitude compared to the overall intraspecific variability across ecosystems. Nevertheless, our simulations provide valuable information to explore the relevance of variations in blade biomechanical traits to the mechanisms that drive flow-seagrass interactions in a more general context.

To assess the impact of biomass height on seagrass productivity, we estimated the averaged light irradiance availability for a shoot in each case investigated. Using the light irradiance data provided by DHI and Equation 8 we estimated the vertical light attenuation coefficient  $K_d$ , which describes how the light irradiance decreases with the water depth. Then, we calculated the light irradiance available to a shoot by integrating the light irradiance available to all shoot elements (see Section 2.4.1) depending on their height in the water column and neglecting potential self-shading effects. For these calculations we assumed the water depth to be equal to the spatially averaged water depth across the lagoon, i.e. 4 m. To calculate the downward light irradiance available to an element we used the monotonical exponential decrease model for downward light irradiance (Kirk, 1994), i.e.:

$$E_d(z) = E_d(0)e^{-K_d z}, \quad (8)$$

where  $E_d(z)$  is the downward light irradiance at a water depth  $z$ ,  $E_d(0)$  is the downward light irradiance at the water surface, and  $K_d$  is the vertical light attenuation coefficient.

Exposure to laboratory conditions with high nutrient levels for 9 days has a significant effect on flow-seagrass interactions: biomass height is decreased and the mean drag force is lowered by 27% (Figures 3 and 4), whereas light irradiance availability does not vary (for the laboratory case it is estimated as 0.054 mol<sub>photon</sub>/d). This result was somewhat expected given the considerable effect of high nutrient levels on the Young's modulus of blades. Hence, our findings show that flow-seagrass interactions can vary in a matter of days depending on the water quality. Bearing in mind that high nutrient levels strongly decrease the survival of *Z. noltii* in a 8-weeks time span (La Nafie et al., 2012), we may speculate that reductions in the biomass height and mean drag force—caused by a lower flexural rigidity—represent the first indications of seagrass decay. In the context of seagrass being used in flume facilities, this indicates that the hydrodynamic performance of shoots is not representative of natural conditions if the shoots have been stored in suboptimal laboratory conditions for several days.

Biomechanical variability induced by seasonality has considerable effects on seagrass response to hydrodynamic forcing, influencing both plant posture and drag force. On the one hand, summer blades have their photosynthetically active biomass shifted closer to the water surface, with beneficial effects for their energy balance. According to our crude approximation, light irradiance available to a plant in summer is about twice as much as light irradiance available in spring (0.120 mol photon/d vs. 0.055 mol photon/d); even considering the same ambient light conditions (i.e. same light irradiance at the water surface), summer plants potentially capture about 34% more light than spring plants (0.073 mol<sub>photon</sub>/d). On the other hand, this

positive effect comes at the price of exposing summer plants to higher mean drag forces (about 45% higher than spring plants at the same mean flow velocity). Even though in the context of the natural conditions at the site (i.e. combined wave-current flow) the magnitude of these differences may vary, we expect the overall trends to hold true regardless. In particular, the variance of the parameters considered for assessing flow-seagrass interactions should increase considerably, but the mean values should be less affected because of the oscillatory nature of wave motion.

Also simulations accounting for within-plant biomechanical heterogeneity show a difference in seagrass response to hydrodynamic forcing when compared with the spring case (Table 3). These cases are particularly useful for inferring the mechanisms driving flow-seagrass interactions. The effect on light availability is small, with light irradiance available in the ranked and heterogeneous cases equal to 0.057 mol photon/d and 0.055 mol photon/d, respectively (in the spring case it is 0.055 mol photon/d). The ranked case performs similarly to the spring case in terms of deflected height but the mean drag force is reduced by 10%. This suggests that seagrass response to hydrodynamic forcing is also regulated by blade rank, whose characteristic biomechanics grant seagrass shoots a substantial moderation in the drag force with respect to idealized shoots made up by blades with the same biomechanical traits (Table 3). Simulations accounting for heterogeneity associated with position along blades in both spring and summer (see supporting information) specimens show negligible differences from the reference cases. Based on this, we argue that within-blade heterogeneity does not impact flow-seagrass interactions as significantly as the other factors investigated in the current study. This contrasts with Marjoribanks & Paul, (in press) who showed that accounting for this heterogeneity in biomechanics can alter the drag on saltmarsh vegetation by up to 25%. We suggest this is due to the much lower values for the mean and along-blade variation in flexural rigidity observed in seagrasses compared to saltmarsh vegetation.

Our work characterizes the temporal variability and within-plant heterogeneity in biomechanical traits of *Z. marina* blades and their roles in flow-seagrass interactions. The idealized hydrodynamic forcing considered in our model is a simplified scenario of the forcing experienced by seagrasses at the collection site. A uniform flow scenario is reasonable for individual plants (Luhar & Nepf, 2011) because the boundary layer is very thin and flow nonuniformity interests only the stiffest part of the plant (i.e. the sheath bundle). However, we do expect that the temporal variability characteristic of combined wave-current flows may have a strong impact on flow-seagrass interactions, facilitating dynamic blade reconfiguration and, hence, enhancing the variability of the hydrodynamic parameters considered in this work. For example, we note that, due to the simplicity of the flow model, blade profiles displayed in Figure 3 are almost straight with no flapping, contrary to what has been reported in earlier works with seagrasses (Abdelrhman, 2007; Lei & Nepf, 2019a). In this context, it is also likely that interactions between blades would have a role in flow-seagrass interactions.

We recall here that seagrass morphology is fairly simple, especially when compared to other types of aquatic vegetation, therefore within-plant heterogeneity is likely to have a more significant role in defining the interactions with the flow of other vegetation types. In this sense, seagrass represents a benchmark case for vegetation with more complex morphology. Ability to replicate temporal variability in biomechanics and within-plant heterogeneity may be a key aspect in unlocking further advancements in our understanding of flow-vegetation interactions.

### 4.3. Some Recommendations for Future Experiments on Seagrass

Given the strong biomechanical variability of seagrass, we recommend future seagrass models to be designed using the biomechanical traits of specimens exposed to the environmental conditions of interest. Similar to what reported by Vettori and Nikora (2020) for macroalgae, this aspect is crucial for attaining accurate results, as seagrass adapted to different conditions can vary significantly both in terms of biological (e.g., light availability) and hydrodynamic (e.g., drag force) performance. Our results indicate that future models should also account for blade ranks, as their influence on drag force is substantial, but could neglect along-blade heterogeneity. Concerning the use of live seagrass plants in laboratories, based on the “laboratory” case we recommend that seagrasses are stored in optimal environmental conditions or used within 48 h of collection to prevent potential biomechanical variations, which we demonstrate can occur over a short period, that can bias experimental results.

## 5. Conclusions

In this work we characterize temporal variability and within-plant heterogeneity in blade biomechanics of *Z. marina* from the Rødsand lagoon (Denmark) and their effects on flow-seagrass interactions. Biomechanical traits were measured from seagrass shoots collected in late summer and early spring, then they were used to parameterize the numerical model of flow-seagrass interactions. The structural model simulates seagrass response to an idealized steady uniform flow and includes heterogeneity in the biomechanical traits within a seagrass plant associated with blade rank and position along blades.

In partial accordance to findings of previous works, we report that seasonality and high nutrient levels strongly affect blade biomechanics. Compared to blades from late summer, spring blades are smaller in size, less rigid and buoyant, but the number of photosynthetically active blades remains constant. Short-term exposure to nutrient-rich water triggers a reduction in the blade's Young's modulus at bending that becomes already significant after 2–3 days. Flow-seagrass interactions are considerably affected by biomechanical variation associated with seasonality both in terms of the drag force and light availability: summer plants can potentially capture more light, while spring plants are more efficient at avoiding the drag force. This suggests that temporal variability in seagrass blade biomechanics driven by environmental conditions may play a critical role in plant response to the flow.

The findings of this study demonstrate that blade biomechanics are heterogeneous within a given plant, varying with blade rank and position along blades. Seagrass biomechanical traits vary with the age of the tissues: blade size, material density, and stiffness increase with blade rank up to blade rank 4, at which point biomechanical properties seem to stabilize; and blades are stiffer at the top than at the bottom. Surprisingly, within-plant heterogeneity associated with blade rank causes a reduction in the drag force experienced by a seagrass shoot without affecting light availability. It is possible that this heterogeneity is an important factor contributing to optimal seagrass response to flow conditions compared to structures with homogeneous biomechanical properties. The effects of temporal variability and within-plant heterogeneity in biomechanical traits should be characterized further in hydraulic conditions which better replicate natural scenarios (e.g., turbulent or oscillatory flows) and with other types of (aquatic) vegetation.

Based on the results of the current study we conclude that: (i) when conducting laboratory experiments with live seagrass, shoots should be exposed to optimal conditions or used within 48 h of collection to prevent potential bias in the results; (ii) temporal variability in blade biomechanics associated with seasonality has an important role in controlling flow-seagrass interactions; and (iii) within-plant biomechanical heterogeneity associated with blade rank may represent an efficient strategy to reduce the drag force.

## Data Availability Statement

Data supporting the conclusions of this publication can be found in the open access repository Zenodo at the following link: <https://zenodo.org/record/3755315>

## References

- Abdelrhman, M. A. (2007). Modeling coupling between eelgrass *Zostera marina* and water flow. *Marine Ecology Progress Series*, 338(May 2007), 81–96. <https://doi.org/10.3354/meps338081>
- Abdolahpour, M., Ghisalberti, M., McMahon, K., & Lavery, P. (2018). *The impact of flexibility on flow, turbulence, and vertical mixing in coastal canopies* (pp. 1–16). *Limnology and Oceanography*. <https://doi.org/10.1002/lno.11008>
- Adams, M. P., Hovey, K. K., Hipsey, M. R., Bruce, L. C., Ghisalberti, M., Lowe, R. J., et al. (2016). Feedback between sediment and light for seagrass: Where is it important? *Limnology & Oceanography*, 61(6), 1937–1955.
- Baker, N. R. (2008). Chlorophyll fluorescence: a probe of photosynthesis in vivo. *Annual Review of Plant Biology*, 59, 89–113. <https://doi.org/10.1146/annurev.arplant.59.032607.092759>
- Bakker, E. S., Wood, K. A., Pagès, J. F., Veen, G. F. C., Christianen, M. J. A., Santamaría, L., et al. (2016). Herbivory on freshwater and marine macrophytes: a review and perspective. *Aquatic Botany*, 135, 18–36. <https://doi.org/10.1016/j.aquabot.2016.04.008>
- Barbier, E. B., Hacker, S. D., Kennedy, C., Koch, E. W., Stier, A. C., & Silliman, B. R. (2011). The value of estuarine and coastal ecosystem services. *Ecological Monographs*, 81(2), 169–193. <https://doi.org/10.1890/10-1510.1>
- Burkholder, J. M., Mason, K. M., & Glasgow, H. B., Jr (1992). Water-column nitrate enrichment promotes decline of eelgrass *Zostera marina*: evidence from seasonal mesocosm experiments. *Marine Ecology Progress Series*, 81(2), 163–178.
- Dijkstra, J. T., & Uittenbogaard, R. E. (2010). Modeling the interaction between flow and highly flexible aquatic vegetation. *Water Resources Research*, 46(12), 1–14. <https://doi.org/10.1029/2010WR009246>

## Acknowledgments

D. Vettori would like to thank the European Community's Horizon 2020 Program through the grant to the budget of the Integrated Infrastructure Initiative HYDRALAB+, Contract no. 654110 for supporting this study. D. Vettori gratefully acknowledges: Anne Lise Middelboe for arranging collection and transport of seagrass specimens; Kadri Kuusemäe for providing data of environmental conditions in the Rødsand lagoon; DHI for providing onsite measurements of hydrodynamic conditions in the lagoon; Leonie Akervo and Jasper Dijkstra for help with onsite biomechanical measurements in summer 2017; and Christopher Jones for shooting microscope photos used for Figure 5. Very insightful comments provided by two anonymous reviewers and the Associate Editor helped to improve the quality of the paper.

- Duarte, C. M., Losada, I. J., Hendriks, I. E., Mazarrasa, I., & Marbà, N. (2013). The role of coastal plant communities for climate change mitigation and adaptation. *Nature Climate Change*, 3(11), 961. <https://doi.org/10.1038/NCLIMATE1970>
- Durako, M. J., & Kunzelman, J. I. (2002). Photosynthetic characteristics of *Thalassia testudinum* measured in situ by pulse-amplitude modulated (PAM) fluorometry: methodological and scale-based considerations. *Aquatic Botany*, 73, 173–185. [https://doi.org/10.1016/S0304-3770\(02\)00020-7](https://doi.org/10.1016/S0304-3770(02)00020-7)
- Fehmarnbelt Fixed Link EIA (FEMA). (2013). *Marine Fauna and Flora – Baseline Benthic Flora of the Fehmarnbelt area* Vol. (I. Report No. E2TR0020.
- Folkard, A. M. (2005). Hydrodynamics of model *Posidonia oceanica* patches in shallow water. *Limnology & Oceanography*, 50(5), 1592–1600. <https://doi.org/10.4319/lo.2005.50.5.1592>
- Gacia, E., & Duarte, C. M. (2001). Sediment retention by a Mediterranean *Posidonia oceanica* meadow: the balance between deposition and resuspension. *Estuarine, Coastal and Shelf Science*, 52(4), 505–514. <https://doi.org/10.1006/ecss.2000.0753>
- Hansen, J. C. R., & Reidenbach, M. A. (2012). Wave and tidally driven flows in eelgrass beds and their effect on sediment suspension. *Marine Ecology Progress Series*, 448, 271–287. <https://doi.org/10.3354/meps09225>
- Hemminga, M. A., & Duarte, C. M. (2000). *Seagrass ecology*. Cambridge, UK: Cambridge University Press.
- Henry, P.-Y. (2014). Bending properties of a macroalga: Adaptation of Peirce's cantilever test for in situ measurements of *Laminaria digitata* (Laminariaceae). *American Journal of Botany*, 101(6), 1050–1055. <https://doi.org/10.3732/ajb.1400163>
- Hily, C., Raffin, C., Brun, A., & den Hartog, C. (2002). Spatio-temporal variability of wasting disease symptoms in eelgrass meadows of Brittany (France). *Aquatic Botany*, 72(1), 37–53. [https://doi.org/10.1016/S0304-3770\(01\)00195-4](https://doi.org/10.1016/S0304-3770(01)00195-4)
- Infantes, E., Orfila, A., Simarro, G., Terrados, J., Luhar, M., & Nepf, H. M. (2012). Effect of a seagrass (*Posidonia oceanica*) meadow on wave propagation. *Marine Ecology Progress Series*, 456, 63–72. <https://doi.org/10.3354/meps09754>
- James, R. K., Silva, R., van Tussenbroek, B. I., Escudero-Castillo, M., Mariño-Tapia, I., Dijkstra, H. A., et al. (2019). Maintaining tropical beaches with seagrass and algae: a promising alternative to engineering solutions. *BioScience*, 69(2), 136–142. <https://doi.org/10.1093/biosci/biy154>
- Kirk, J. T. O. (1994). *Light and photosynthesis in aquatic ecosystems*. Cambridge University Press.
- Kuo, J., & Den Hartog, C. (2007). Seagrass morphology, anatomy, and ultrastructure. In A. W. D. Larkum, R. J. Orth, & C. Duarte (Eds.), *Seagrasses: Biology, Ecology and Conservation* (pp. 51–87). Dordrecht: Springer. [https://doi.org/10.1007/978-1-4020-2983-7\\_3](https://doi.org/10.1007/978-1-4020-2983-7_3)
- Lamb, J. B., Van De Water, J. A. J. M., Bourne, D. G., Altier, C., Hein, M. Y., Fiorenza, E. A., et al. (2017). Seagrass ecosystems reduce exposure to bacterial pathogens of humans, fishes, and invertebrates. *Science*, 355(6326), 731–733.
- Leclercq, T., & de Langre, E. (2016). Drag reduction by elastic reconfiguration of non-uniform beams in non-uniform flows. *Journal of Fluids and Structures*, 60, 114–129. <https://doi.org/10.1016/j.jfluidstructs.2015.10.007>
- Lei, J., & Nepf, H. M. (2019a). Blade dynamics in combined waves and current. *Journal of Fluids and Structures*, 87, 137–149. <https://doi.org/10.1016/j.jfluidstructs.2019.03.020>
- Lei, J., & Nepf, H. M. (2019b). Wave damping by flexible vegetation: Connecting individual blade dynamics to the meadow scale. *Coastal Engineering*, 147, 138–148.
- de los Santos, C. B., Brun, F. G., Vergara, J. J., & Pérez-Lloréns, J. L. (2013). New aspect in seagrass acclimation: leaf mechanical properties vary spatially and seasonally in the temperate species *Cymodocea nodosa* Ucria (Ascherson). *Marine Biology*, 160(5), 1083–1093. <https://doi.org/10.1007/s00227-012-2159-3>
- de los Santos, C. B., Vicencio-Rammsy, B., Lepoint, G., Remy, F., Bouma, T. J., & Gobert, S. (2016). Ontogenic variation and effect of collection procedure on leaf biomechanical properties of Mediterranean seagrass *Posidonia oceanica* (L.) Delile. *Marine Ecology*, 37(4), 750–759.
- Luhar, M., & Nepf, H. M. (2011). Flow-induced reconfiguration of buoyant and flexible aquatic vegetation. *Limnology & Oceanography*, 56(6), 2003–2017. <https://doi.org/10.4319/lo.2011.56.6.2003>
- Marjoribanks, T. I., & Paul, M. Modeling flow-induced reconfiguration of variable rigidity aquatic vegetation. *Journal of Hydraulic Research*. (in press) <https://doi.org/10.1080/00221686.2020.1866693>
- Marjoribanks, T. I., Lague, D., Hardy, R. J., Boothroyd, R. J., Leroux, J., Mony, C., & Puijalon, S. (2019). Flexural rigidity and shoot reconfiguration determine wake length behind saltmarsh vegetation patches. *Journal of Geophysical Research: Earth Surface*, 124, 2176–2196. <https://doi.org/10.1029/2019JF005012>
- McLeod, E., Chmura, G. L., Bouillon, S., Salm, R., Björk, M., Duarte, C. M., et al. (2011). A blueprint for blue carbon: toward an improved understanding of the role of vegetated coastal habitats in sequestering CO<sub>2</sub>. *Frontiers in Ecology and the Environment*, 9(10), 552–560. <https://doi.org/10.1890/110004>
- Moore, K. A., & Wetzel, R. L. (2000). Seasonal variations in eelgrass (*Zostera marina* L.) responses to nutrient enrichment and reduced light availability in experimental ecosystems. *Journal of Experimental Marine Biology and Ecology*, 244, 1–28.
- Murchie, E. H., & Lawson, T. (2013). Chlorophyll fluorescence analysis: a guide to good practice and understanding some new applications. *Journal of Experimental Botany*, 64(13), 3983–3998. <https://doi.org/10.1093/jxb/ert208>
- La Nafie, Y. A., Carmen, B., Brun, F. G., Mashoreng, S., van Katwijk, M. M., & Bouma, T. J. (2013). Biomechanical response of two fast-growing tropical seagrass species subjected to in situ shading and sediment fertilization. *Journal of Experimental Marine Biology and Ecology*, 446, 186–193. <https://doi.org/10.1016/j.jembe.2013.05.020>
- La Nafie, Y. A., de los Santos, C. B., Brun, F. G., van Katwijk, M. M., & Bouma, T. J. (2012). Waves and high nutrient loads jointly decrease survival and separately affect morphological and biomechanical properties in the seagrass *Zostera noltii*. *Limnology & Oceanography*, 57(6), 1664–1672. <https://doi.org/10.4319/lo.2012.57.6.1664>
- Neckles, H. A., Wetzel, R. L., & Orth, R. J. (1993). Relative effects of nutrient enrichment and grazing on epiphyte-macrophyte (*Zostera marina* L.) dynamics. *Oecologia*, 93(2), 285–295. <https://doi.org/10.1007/BF00317683>
- Neild, S. A., Mcfadden, P. D., & Williams, M. S. (2001). A discrete model of a vibrating beam using a time-stepping approach. *Journal of Sound and Vibration*, 239(1), 99–121.
- Niklas, K. J. (1992). *Plant biomechanics: An engineering approach to plant form and function*. Chicago: University of Chicago Press.
- Niklas, K. J., & Spatz, H.-C. (2012). *Plant physics*. Chicago: University of Chicago Press.
- Ochieng, C. A., Short, F. T., & Walker, D. I. (2010). Photosynthetic and morphological responses of eelgrass (*Zostera marina* L.) to a gradient of light conditions. *Journal of Experimental Marine Biology and Ecology*, 382(2), 117–124. <https://doi.org/10.1016/j.jembe.2009.11.007>
- Paul, M., & Amos, C. L. (2011). Spatial and seasonal variation in wave attenuation over *Zostera noltii*. *Journal of Geophysical Research: Oceans*, 116, C08019. <https://doi.org/10.1029/2010JC006797>
- Paul, M., & de los Santos, C. B. (2019). Variation in flexural, morphological, and biochemical leaf properties of eelgrass (*Zostera marina*) along the European Atlantic climate regions. *Marine Biology*, 166(10), 127.

- Peirce, F. T. (1930). The handle of cloth as a measurable quantity. *Journal of the Textile Institute Transactions*, 21(9), T377–T416. <https://doi.org/10.1080/19447023008661529>
- Ralph, P. J., & Burchett, M. D. (1995). Photosynthetic responses of the seagrass *Halophila ovalis* (R. Br.) Hook. f. to high irradiance stress, using chlorophyll a fluorescence. *Aquatic Botany*, 51, 55–66.
- Ralph, P. J., & Gademann, R. (2005). Rapid light curves: A powerful tool to assess photosynthetic activity. *Aquatic Botany*, 82, 222–237. <https://doi.org/10.1016/j.aquabot.2005.02.006>
- Ralph, P. J., Durako, M. J., Enriquez, S., Collier, C. J., & Doblin, M. A. (2007). Impact of light limitation on seagrasses. *Journal of Experimental Marine Biology and Ecology*, 350, 176–193. <https://doi.org/10.1016/j.jembe.2007.06.017>
- Soissons, L. M., van Katwijk, M. M., Peralta, G., Brun, F. G., Cardoso, P. G., Grilo, T. F., et al. (2018). Seasonal and latitudinal variation in seagrass mechanical traits across Europe: The influence of local nutrient status and morphometric plasticity. *Limnology & Oceanography*, 63(1), 37–46. <https://doi.org/10.1002/lno.10611>
- Stratigaki, V., Manca, E., Prinos, P., Losada, I. J., Lara, J. L., Sclavo, M., et al. (2011). Large-scale experiments on wave propagation over *Posidonia oceanica*. *Journal of Hydraulic Research*, 49(sup1), 31–43. <https://doi.org/10.1080/00221686.2011.583388>
- Taylor, G. I. (1952). Analysis of the swimming of long and narrow animals. In *Proceedings of the Royal Society of London. Series A. Mathematical and physical Sciences* Vol. (214 (pp. 1117158–183). <https://doi.org/10.1098/rspa.1952.0159>
- Vettori, D., & Nikora, V. (2017). Morphological and mechanical properties of blades of *Saccharina latissima*. *Estuarine, Coastal and Shelf Science*, 196, 1–9. <https://doi.org/10.1016/j.ecss.2017.06.033>
- Vettori, D., & Nikora, V. (2020). Hydrodynamic performance of vegetation surrogates in hydraulic studies: a comparative analysis of seaweed blades and their physical models. *Journal of Hydraulic Research*, 58(2), 248–261. <https://doi.org/10.1080/00221686.2018.1562999>
- Vettori, D., & Rice, S. P. (2020). Implications of environmental conditions for health status and biomechanics of freshwater macrophytes in hydraulic laboratories. *Journal of Ecohydraulics*, 5(1), 71–83. <https://doi.org/10.1080/24705357.2019.1669496>
- Vogel, S. (1981). *Life in moving fluids: The physical biology of flow*. University of Chicago Press. [https://doi.org/10.1016/0022-0981\(96\)02487-2](https://doi.org/10.1016/0022-0981(96)02487-2)